

RESEARCH

Open Access



High-resolution detection of quantitative trait loci for seven important yield-related traits in wheat (*Triticum aestivum* L.) using a high-density SLAF-seq genetic map

Tao Li^{1,2,3}, Qiao Li¹, Jinhui Wang¹, Zhao Yang¹, Yanyan Tang¹, Yan Su¹, Juanyu Zhang¹, Xvebing Qiu¹, Xi Pu¹, Zhifen Pan¹, Haili Zhang¹, Junjun Liang¹, Zehou Liu⁴, Jun Li⁴, Wuyun Yan³, Maoqun Yu¹, Hai Long¹, Yuming Wei^{2,3} and Guangbing Deng^{1*}

Abstract

Background: Yield-related traits including thousand grain weight (TGW), grain number per spike (GNS), grain width (GW), grain length (GL), plant height (PH), spike length (SL), and spikelet number per spike (SNS) are greatly associated with grain yield of wheat (*Triticum aestivum* L.). To detect quantitative trait loci (QTL) associated with them, 193 recombinant inbred lines derived from two elite winter wheat varieties Chuanmai42 and Chuanmai39 were employed to perform QTL mapping in six/eight environments.

Results: A total of 30 QTLs on chromosomes 1A, 1B, 1D, 2A, 2B, 2D, 3A, 4A, 5A, 5B, 6A, 6D, 7A, 7B and 7D were identified. Among them, six major QTLs *QTgw.cib-6A.1*, *QTgw.cib-6A.2*, *QGw.cib-6A*, *QGl.cib-3A*, *QGl.cib-6A*, and *QSl.cib-2D* explaining 5.96–23.75% of the phenotypic variance were detected in multi-environments and showed strong and stable effects on corresponding traits. Three QTL clusters on chromosomes 2D and 6A containing 10 QTLs were also detected, which showed significant pleiotropic effects on multiple traits. Additionally, three Kompetitive Allele Specific PCR (KASP) markers linked with five of these major QTLs were developed. Candidate genes of *QTgw.cib-6A.1/QGl.cib-6A* and *QGl.cib-3A* were analyzed based on the spatiotemporal expression patterns, gene annotation, and orthologous search.

Conclusions: Six major QTLs for TGW, GL, GW and SL were detected. Three KASP markers linked with five of these major QTLs were developed. These QTLs and KASP markers will be useful for elucidating the genetic architecture of grain yield and developing new wheat varieties with high and stable yield in wheat.

Keywords: Wheat, Yield, Yield-related traits, Specific-locus amplified fragment (SLAF), Linkage analysis

Background

Common wheat (*Triticum aestivum* L.) is one of the three major crops worldwide and provides approximately 30% of global grain production and 20% of the calories consumed for humans [1]. Due to ongoing decrease of the global arable cultivated land area and increase of the population, the current rate of wheat yield increase will be insufficient to meet the future demand. Thus, breeding

*Correspondence: denggb@cib.ac.cn

¹ Chengdu Institute of Biology, Chinese Academy of Sciences, Chengdu 610041, China

Full list of author information is available at the end of the article



© The Author(s) 2022. **Open Access** This article is licensed under a Creative Commons Attribution 4.0 International License, which permits use, sharing, adaptation, distribution and reproduction in any medium or format, as long as you give appropriate credit to the original author(s) and the source, provide a link to the Creative Commons licence, and indicate if changes were made. The images or other third party material in this article are included in the article's Creative Commons licence, unless indicated otherwise in a credit line to the material. If material is not included in the article's Creative Commons licence and your intended use is not permitted by statutory regulation or exceeds the permitted use, you will need to obtain permission directly from the copyright holder. To view a copy of this licence, visit <http://creativecommons.org/licenses/by/4.0/>. The Creative Commons Public Domain Dedication waiver (<http://creativecommons.org/publicdomain/zero/1.0/>) applies to the data made available in this article, unless otherwise stated in a credit line to the data.

of high-yield wheat varieties to ensure future global food and nutrition security is an important target of the modern wheat breeding programs [2].

Wheat yield is a complex quantitative trait controlled by multiple genes and significantly influenced by interacting genetic and environmental factors [3, 4]. By contrast, yield components including thousand grain weight (TGW), grain number per spike (GNS), grain width (GW), grain length (GL), plant height (PH), spike length (SL) and spikelet number per spike (SNS) typically show higher heritability than that of the yield [5–7]. Therefore, targeting these traits and identifying the related genes or quantitative trait loci (QTL) is an important approach to improve grain yield potential in wheat.

The molecular cloning of genes associated with wheat yield is difficult owing to wheat's huge and complicated genome. To date, only a few genes associated with grain yield have been cloned in wheat. For example, the application of semi-dwarfing genes *Rht-B1b* and *Rht-D1b* not only effectively improve the lodging resistance but also improve the harvest index, resulting in increasing yield since the 1970s [8–10]. The vernalization insensitive alleles of *Vrn-1* (*Vrn-A1*, *Vrn-B1*, and *Vrn-D1*) shorten both the vegetative and the reproductive stages and have considerable impact on spike morphological traits [11, 12]. The grain-shape gene *TasgD1* encoding a Ser/Thr protein kinase glycogen synthase kinase3 and independently control semispherical grain trait [13]. A jasmonic acid synthetic gene keto-acyl thiolase 2B was cloned in a TGW mutant, showing significant effects on TGW and GW [14]. Additionally, homologous cloning is an effective approach to characterize gene in wheat. As of today more than 20 genes related to yield have been isolated through homologous cloning approach, including *WFZP*, *WAP01*, *TaGW7*, *TaGW2*, *TaCKX6-D1*, *TaTGW6*, *TaGASR7*, *TaGL3* and *TaGS-D1* et al [15–23].

Quantitative trait loci (QTL) mapping provides an effective approach to dissect the genetic architecture of complex quantitative traits. Over the past decades, numerous QTLs associated with yield or yield-related traits have been identified on all wheat chromosomes [3, 4, 11, 24–30]. For example, *Rht8* located on chromosome 2DS was closely linked with marker *xfdc53* and reduced plant height by 10% [31]; *Rht25* on wheat chromosome arm 6AS showed pleiotropic effects on coleoptile length, heading date, SL, SNS and grain weight [32]. Two major QTLs for grain size and weight were detected on chromosome 4B, which together explained 46.3% of the phenotypic variance [33, 34]. Five stable QTLs for PH, SL and HD on chromosomes 1A, 2A, 2D and 6A were detected in an introgression line population [35]. Twelve major genomic regions with stable QTL controlling yield-related traits were detected on chromosomes 1B, 2A, 2B,

2D, 3A, 4A, 4B, 4D, 5A, 6A, and 7A [1]. However, among these QTLs reported previously, few of them were stably detected in multi-environments, which greatly restrict their potential utilization in marker-assisted selection (MAS) in breeding programs.

With the development of high-throughput sequencing technology, Single nucleotide polymorphisms (SNP) markers have been widely applied to construct high-density genetic maps for QTL mapping, due to their extensive and intensive distribution throughout genomes in many crops [3, 36–38]. Specific-locus amplified fragment sequencing (SLAF-seq) was developed for economic and efficient high-throughput SNP discovery through restriction-site associated DNA tag sequencing (RAD-seq), which can provide abundant InDel and SNP markers to construct high-density genetic map [39–41].

In the present study, a high-resolution genetic map was constructed in a recombinant inbred line (RIL) population derived from two elite winter wheat varieties Chuanmai42 (CM42) and Chuanmai39 (CM39) based on SLAF-seq (Table S1, S2) [42]. Seven traits including TGW, GW, GL, PH, GNS, SL and SNS were assessed in multi-environments to detect potential major and stable QTL, which will lay out a foundation for further study on fine mapping and cloning of the underlying key genes for wheat yield.

Results

Phenotypic variation

The phenotypic analysis showed that CM42 had higher trait values for TGW, GW, GL, GNS, PH and SL than those of CM39 in each of environments and the best linear unbiased prediction (BLUP) datasets (Table 1). In the RIL population, seven yield-related traits showed wide and significant variations in all environments and the BLUP datasets (Table 1). Of them, the TGW ranged from 20.81 to 72.7 gram (g), the GW ranged from 2.6 to 4.21 millimeter (mm), the GL ranged from 5.88 to 8.81 mm, the PH ranged from 65.08 to 148.3 centimeter (cm), the GNS ranged from 24 to 84.6, the SL ranged from 6.65 to 18.17 cm, and the SNS ranged from 15.83 to 27, respectively (Table 1). The BLUP datasets of all traits showed normal distributions in the RIL lines, which suggested polygenic inheritance of these traits (Fig. 1A). Additionally, the TGW, GL, PH, GNS and SL showed high cross-environment broad-sense heritability of 0.54, 0.6, 0.91, 0.66 and 0.88, respectively (Table 1). Significant and positive correlations ($P < 0.01$) of the seven yield-related traits among all environments and the BLUP datasets were detected, which suggested that these traits were environmentally stable and mainly controlled by genetic factors (Table S3).

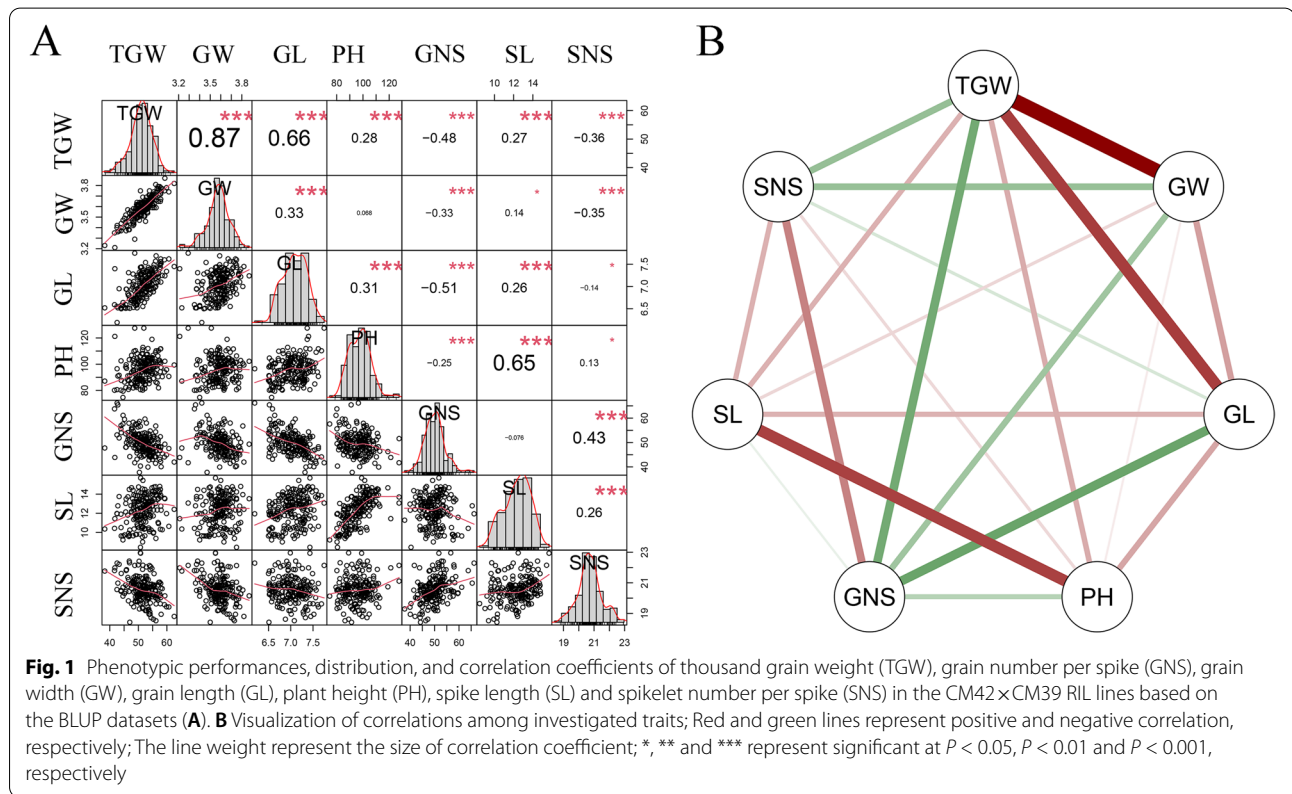
Table 1 Phenotypic variation of the seven yield-related traits, including thousand grain weight (TGW), grain number per spike (GNS), grain width (GW), grain length (GL), plant height (PH), spike length (SL) and spikelet number per spike (SNS), for the parents and the CM42×CM39 RIL lines in different environments

Traits	Environments	Parents		The CM42×CM39 RIL lines					H^2
		CM42	CM39	Range	Mean	SD	CV (%)		
TGW	2017SHF	54	52.94	38.34-70.88	58.57	5.84	9.98	0.54	
	2017SHL	50.64	41.83	20.81-68.14	43.76	9.17	20.95		
	2018SHF	54.79	53.47	40.44-72.7	54.67	5.58	10.2		
	2018SHL	53.06	51.29	37.89-67.33	54.51	5.57	10.22		
	2019SHF	52.4	42.42	32.59-66.54	51.27	5.94	11.59		
	2019SHL	51.05	47.38	23.4-62.74	46.9	6.22	13.27		
	BLUP	52.36	50.44	38.24-62.56	51.65	3.98	7.7		
GW	2017SHF	3.68	3.42	3.19-4.21	3.82	0.16	4.28	0.49	
	2017SHL	3.54	3.31	2.6-4.01	3.38	0.29	8.57		
	2018SHF	3.58	3.53	3.19-4.04	3.69	0.16	4.35		
	2018SHL	3.63	3.61	3.15-3.96	3.65	0.15	4.14		
	2019SHF	3.6	3.16	3-3.9	3.5	0.18	5.21		
	2019SHL	3.56	3.49	2.84-3.99	3.49	0.19	5.37		
	BLUP	3.59	3.51	3.21-3.87	3.59	0.11	3.06		
GL	2017SHF	7.73	7.17	6.78-8.81	7.76	0.41	5.26	0.6	
	2017SHL	6.95	6.53	5.94-7.89	6.86	0.37	5.39		
	2018SHF	6.87	6.72	5.89-7.92	6.95	0.37	5.3		
	2018SHL	7.64	6.55	5.88-7.81	6.85	0.37	5.45		
	2019SHF	7.32	6.43	6-7.71	6.86	0.33	4.84		
	2019SHL	7.22	6.67	6.03-7.71	6.94	0.36	5.15		
	BLUP	7.27	6.98	6.19-7.75	7.04	0.3	4.26		
PH	2016SHF	90.34	89.5	66.5-120.3	91.53	9.5	10.38	0.91	
	2016SHL	89.8	87.2	76-148.3	95.97	10.49	10.93		
	2017SHF	97.67	96.33	81.33-143	103.3	10.65	10.31		
	2017SHL	99	98.8	66.63-121.2	91.39	9.73	10.65		
	2018SHF	91.7	87.08	65.08-131.9	93.9	11.82	12.59		
	2018SHL	94.61	90	70.8-135.4	95.57	11.32	11.84		
	2019SHF	90.05	85.9	69.45-126.8	98.74	9.89	10.02		
	2019SHL	93.33	89.3	78.5-127.4	97.58	8.98	9.21		
	BLUP	93.24	91.91	74.65-127.5	96	9.14	9.52		
GNS	2017SHF	54	52	24-81.2	51.01	10.39	20.38	0.66	
	2017SHL	44.5	43.6	26-77	41.94	8.08	19.27		
	2018SHF	54.6	49.9	31.6-70.8	45.62	6.11	13.4		
	2018SHL	54.5	54.1	35.3-70.8	52.07	7.18	13.78		
	2019SHF	55.7	53.7	35.2-84.6	53.66	8.18	15.24		
	2019SHL	56.5	56.2	35.5-75.8	53.77	7.07	13.15		
	BLUP	53.17	52.44	37.76-66.18	49.85	4.62	9.26		
SL	2016SHF	12.18	9.96	8.67-18	13.09	1.75	13.37	0.88	
	2016SHL	12.1	9	6.65-14	10.53	1.61	15.33		
	2017SHF	13.5	11.5	8.5-17.88	13.04	1.73	13.23		
	2017SHL	13	11.5	8.33-17.67	12.93	1.88	14.51		
	2018SHF	11.85	9.26	7.63-14.93	11.82	1.84	15.54		
	2018SHL	13.02	10.9	7.55-15.7	11.3	1.72	15.18		
	2019SHF	13.71	11.2	8.89-18.17	13.25	1.87	14.15		
	2019SHL	12.4	10.5	8.5-16.3	12.51	1.56	12.51		
	BLUP	12.71	11.6	8.45-15.69	12.31	1.5	12.22		

Table 1 (continued)

Traits	Environments	Parents		The CM42 × CM39 RIL lines				
		CM42	CM39	Range	Mean	SD	CV (%)	H ²
SNS	2017SHF	18.6	19.6	16.2-25	19.58	1.39	7.08	0.4
	2017SHL	21.2	21.2	18-27	21.4	1.63	7.63	
	2018SHF	21.9	21.5	17.7-24.5	21.66	1.13	5.2	
	2018SHL	20.9	20.7	17.9-25.2	21.02	1.22	5.81	
	2019SHF	21.7	21.2	17.9-25	21.29	1.2	5.63	
	2019SHL	17.2	18.1	15.83-21.2	18.35	1.04	5.67	
	BLUP	20.3	20.35	18.42-22.96	20.55	0.84	4.1	

SHF Shifang, SHL Shuangliu, BLUP best linear unbiased prediction, CV coefficient of variation, H² broad-sense heritability



Correlation analyses among different traits

The BLUP datasets of each trait was employed to assess their correlations in the CM42 × CM39 RIL population. TGW had significantly positive correlation with GW, GL, PH and SL, and significantly negative correlation with GNS and SNS ($P < 0.001$) (Fig. 1). GW was significantly and positively correlated with GL ($P < 0.001$), weakly and positively correlated with SL ($P < 0.05$), significantly and negatively correlated with GNS and SNS ($P < 0.001$), and not correlated with PH, respectively (Fig. 1). GL

had significantly positive correlation with PH and SL ($P < 0.001$), significantly negative correlation with GNS ($P < 0.001$), and weakly negative correlation with SNS ($P < 0.05$) (Fig. 1). Significantly positive correlations between PH and SL, GNS and SNS, and SL and SNS ($P < 0.001$), weakly positive correlations between PH and SNS ($P < 0.05$), significantly negative correlations between PH and GNS ($P < 0.001$), and no correlations between GNS and SL were detected, respectively (Fig. 1). Grain weight per spike (GWS) is comprised by TGW and GNS in wheat.

Thus, we further analyzed the correlation between the seven yield-related traits and the GWS. The results showed that GWS was significantly positive and positively correlated with TGW, GW, GL, GNS, SNS and SL ($P < 0.05$), and no correlated with PH (Table S4).

QTL detection

Phenotypic data of the seven yield-related traits in each environment and the BLUP datasets were used for QTL detection, in which the BLUP datasets were treated as an additional environment. A total of 30 QTLs were identified in multi-environments and located on all chromosomes excepting 3B, 3D, 4B, 4D, 5D and 6B (Table 2).

For TGW, two QTLs were detected on chromosomes 6A. *QTgw.cib-6A.1* was detected in two environments and the BLUP datasets, explaining 9.89-16.38% of the phenotypic variance. *QTgw.cib-6A.2* was a major QTL detected in four environments and the BLUP datasets and explained 15.31-23.75% of the phenotypic variance. Alleles of CM42 for the two QTLs contributed to higher TGW (Table 2).

For GW, six QTLs were identified on chromosomes 2A, 2B, 5A, 6A and 7B. Of them, a major QTL *QGw.cib-6A* was identified in five environments and the BLUP datasets, explaining 8.6-23.31% of the GW variation. The allele of CM42 contributed positively to the GW. The rest five minor QTLs were identified in two environments and explained 5.2-9.89% of the GW variation. The favorable alleles of *QGw.cib-2A* and *QGw.cib-5A* were contributed by CM39, and that of *QGw.cib-2B.1*, *QGw.cib-2B.2* and *QGw.cib-7B* were contributed by CM42 (Table 2).

Among the six QTLs for GL, two major QTL *QGL.cib-3A* and *QGL.cib-6A* were identified in five environments and the BLUP datasets, explaining 6.55-11.86% and 5.96-13.11% of the GL variation, respectively. The positive additive effects of the two QTLs on GL were contributed by CM42. The rest four minor QTLs were identified in two or three environments on chromosome 5A, 6D and 7D, explaining 5.17-11.34% of the GL variation. The favorable alleles of *QGL.cib-5A.1*, *QGL.cib-5A.2*, and *QGL.cib-7D* were derived from CM42, and that of *QGL.cib-6D* was derived from CM39 (Table 2).

Among the six QTLs for PH, *QPh.cib-2D* on chromosome 2D was a stable QTL and detected in five environments and the BLUP datasets, explaining 4.54-9.38% of the PH variation. The allele of CM39 contributed to higher PH. The rest five minor QTLs on chromosomes 1A, 4A, 5A, 5B and 6A were detected in two or three environments, explaining 3.8-11.37% of the PH variation. The positive alleles of *QPh.cib-1A* and *QPh.cib-5B* were from CM39, and that of *QPh.cib-4A*, *QPh.cib-5A* and *QPh.cib-6A* were from CM42 (Table 2).

Two minor QTLs for GNS on chromosomes 2D and 6A were detected in two environments and the BLUP datasets and explained 4.97-6.46% and 6.56-7.73% of the GNS variation, respectively. Alleles from CM42 and CM39 at *QGns.cib-2D* and *QGns.cib-6A*, respectively, contributed to positive effects on GNS (Table 2).

For SL, four QTLs were detected on chromosomes 2D, 5A, 5B and 6A. A major QTL *QSl.cib-2D* was detected in eight environments and the BLUP datasets, explaining 6.18-14.89% of the SL variation. *QSl.cib-5B* was a stable QTL and detected in three environments and the BLUP datasets, explaining 3.79-5.96% of the SL variation. Alleles of CM39 for the two QTLs contributed to increase of SL. Two minor QTLs *QSl.cib-5A* and *QSl.cib-6A* were detected in two or three environments, explaining 3.47-7.8% and 5.63-5.9% of the SL variation, respectively. The positive alleles of the two QTLs were contributed by CM42 (Table 2).

Four QTLs for SNS were identified on chromosomes 1B, 1D, 4A and 7A. Of them, *QSns.cib-1B* and *QSns.cib-4A* were detected in three environments and the BLUP datasets, explaining 7.47-16.18% and 2.34-10.46% of the SNS variation, respectively. *QSns.cib-1D* and *QSns.cib-7A* were detected in two environments, explaining 6.77-8.39% and 5.06-8.18% of the SNS variation, respectively. The favorable alleles of *QSns.cib-1B* and *QSns.cib-7A* were contributed by CM39, and that of *QSns.cib-1D* and *QSns.cib-4A* were contributed by CM42 (Table 2).

Effects of major QTL in mapping populations

Six major QTLs *QSl.cib-2D*, *QGL.cib-3A*, *QTgw.cib-6A.1*, *QTgw.cib-6A.2*, *QGw.cib-6A*, and *QGL.cib-6A* were stably identified in multi-environments and the BLUP datasets (Table 2, Fig. 2). Based on the physical position of the flanking markers of them, three Kompetitive Allele Specific PCR (KASP) markers, *K_2D-20925377*, *K_6A-83647812*, and *K_6A-54337781*, tightly linked to *QSl.cib-2D*, *QTgw.cib-6A.1/QGL.cib-6A*, and *QTgw.cib-6A.2/QGw.cib-6A*, respectively, were successfully developed (Table S5, Fig. S1). We further analyzed the effects of these major QTLs on the seven yield-related trait and GWS using the three KASP markers and the flanking markers of *QGL.cib-3A* in the CM42×CM39 RIL population. The results showed that *QSl.cib-2D* significantly affected PH, GNS, SL, SNS and GWS, *QGL.cib-3A* significantly affected TGW, GL, PH, SL and GWS, *QTgw.cib-6A.1/QGL.cib-6A* significantly affected TGW, GW, GL, PH, GNS, SL and GWS, and *QTgw.cib-6A.2/QGw.cib-6A* significantly affected TGW, GW, GL, PH, GNS, SNS and GWS (Fig. 3).

QTL clusters on chromosome 2D and 6A

The QTL cluster on 2D, including three QTLs *QSl.cib-2D*, *QPh.cib-2D* and *QGns.cib-2D*, was co-located between

Table 2 Quantitative trait loci (QTLs) for thousand grain weight (TGW), grain number per spike (GNS), grain width (GW), grain length (GL), plant height (PH), spike length (SL) and spikelet number per spike (SNS) identified across multi-environments in the CM42×CM39 RIL population

Trait	QTL	Env.	Chr.	Interval (cM)
TGW	<i>QTgw.cib-6A.1</i>	18SHF/18SHL/BLUP	6A	41.3-42.46
	<i>QTgw.cib-6A.2</i>	17SHF/18SHL/19SHF/19SHL/BLUP	6A	52.98-59.52
GW	<i>QGw.cib-2A</i>	18SHF/19SHF	2A	14.86-17.08
	<i>QGw.cib-2B.1</i>	19SHF/19SHL	2B	39.6-43.07
	<i>QGw.cib-2B.2</i>	17SHF/BLUP	2B	121.67-121.93
	<i>QGw.cib-5A</i>	17SHF/BLUP	5A	27.76-27.97
	<i>QGw.cib-6A</i>	17SHF/17SHL/18SHL/19SHF/19SHL/BLUP	6A	49.98-58.87
	<i>QGw.cib-7B</i>	18SHF/19SHL	7B	179.93-180.13
	GL	<i>QGl.cib-3A</i>	17SHF/17SHL/18SHL/19SHF/19SHL/BLUP	3A
<i>QGl.cib-5A.1</i>		17SHL/BLUP	5A	3.46-7.55
<i>QGl.cib-5A.2</i>		18SHL/19SHF	5A	86.87-87.49
<i>QGl.cib-6A</i>		17SHF/18SHF/18SHL/19SHF/19SHL/BLUP	6A	42.36-43.4
<i>QGl.cib-6D</i>		18SHL/19SHF/BLUP	6D	76.06-83.69
<i>QGl.cib-7D</i>		17SHF/17SHL/BLUP	7D	32.68-38.76
PH		<i>QPh.cib-1A</i>	16SHF/17SHL/19SHF	1A
	<i>QPh.cib-2D</i>	16SHF/17SHL/18SHF/18SHL/19SHF/BLUP	2D	1.48-5.16
	<i>QPh.cib-4A</i>	16SHF/17SHL	4A	82.78-83.05
	<i>QPh.cib-5A</i>	17SHF/19SHL/BLUP	5A	126.27-126.52
	<i>QPh.cib-5B</i>	16SHF/17SHL	5B	134.43-134.74
	<i>QPh.cib-6A</i>	16SHF/17SHL/19SHF	6A	54.61-54.76
	GNS	<i>QGns.cib-2D</i>	18SHF/19SHF/BLUP	2D
<i>QGns.cib-6A</i>		18SHL/19SHF/BLUP	6A	56.45-59.52
SL	<i>QSl.cib-2D</i>	16SHF/16SHL/17SHF/17SHL/18SHF/18SHL/19SHF/19SHL/BLUP	2D	1.48-5.16
	<i>QSl.cib-5A</i>	18SHL/19SHF/BLUP	5A	17.71-21.48
	<i>QSl.cib-5B</i>	16SHF/16SHL/17SHF/BLUP	5B	40.07-40.38
	<i>QSl.cib-6A</i>	19SHF/BLUP	6A	58.87-64.37
SNS	<i>QSns.cib-1B</i>	17SHF/18SHL/19SHF/BLUP	1B	28.8-33.3
	<i>QSns.cib-1D</i>	17SHL/BLUP	1D	146.67-148.82
	<i>QSns.cib-4A</i>	17SHF/18SHL/19SHF/BLUP	4A	72.98-81.71
	<i>QSns.cib-7A</i>	19SHF/19SHL	7A	81.76-85.42

Table 2 (continued)

Trait	Flanking Markers	LOD	PVE(%)	Add
TGW	Marker87546-Marker87736	6.17/8.03/4.44	13.49/16.38/9.89	-1.89/-2/-1.04
	Marker90290-Marker91587	9.48/7.95/7.27/10.52/9.62	20.39/16.68/15.31/20.51/23.75	-2.58/-2.06/-2.36/-2.88/-1.65
GW	Marker26336-Marker26958	5.48/2.76	9.51/5.81	0.05/0.04
	Marker29502-Marker29525	2.66/4.09	5.46/6.62	-0.04/-0.05
	Marker34419-Marker34417	3.83/3.7	5.2/5.2	-0.04/-0.03
	Marker70243-Marker70216	3.91/4.73	5.29/6.72	0.04/0.03
	Marker90210-Marker91133	13.09/4.95/8.93/4.02/5.8/14.53	19.87/8.92/19.17/8.6/10.1/23.31	-0.08/-0.09/-0.07/-0.05/-0.06/-0.06
	Marker111000-Marker110965	5.36/5.98	9.07/9.89	-0.05/-0.06
GL	Marker40793-Marker40901	5.31/2.97/6.1/5.69/3.87/5.68	11.86/6.55/10.17/10.31/7.37/9.54	-0.13/-0.08/-0.12/-0.1/-0.09/-0.09
	Marker69377-Marker69395	2.83/3.66	6.28/6.26	-0.08/-0.07
	Marker71923-Marker71919	3.79/3.82	6.13/6.76	-0.09/-0.08
	Marker87807-Marker87738	5.32/4.62/7.72/3.39/5.37/7.41	11.85/10.15/13.11/5.96/10.37/12.7	-0.13/-0.12/-0.13/-0.08/-0.11/-0.1
	Marker99119-Marker99140	4.17/5/3.17	6.95/8.98/5.17	0.1/0.1/0.06
	Marker111521-Marker111597	3/4.64/6.19	6.63/11.34/10.49	-0.09/-0.11/-0.09
PH	Marker5758-Marker6328	5.58/6.07/3.64	7.62/7.53/5.87	2.96/3.03/2.65
	Marker35344-Marker35422	3.42/4.31/3/4.7/3.14/2.56	4.54/5.23/6.73/9.38/5.03/6.2	2.29/2.53/3/3.72/2.46/2.31
	Marker57956-Marker57959	4.76/5.71	6.43/7.05	-2.73/-2.95
	Marker72631-Marker72950	3.02/2.91/2.52	7.18/7.03/5.62	-2.8/-2.32/-2.2
	Marker83905-Marker83879	3.07/3.18	4.07/3.8	2.17/2.16
	Marker90459-Marker90388	6.13/8.86/5.6	8.42/11.37/9.25	-3.24/-3.88/-3.46
GNS	Marker35164-Marker35422	2.57/2.63/4.73	5.73/4.97/6.46	-1.44/-1.93/-1.27
	Marker90628-Marker91587	3.35/3.83/4.91	7.73/7.46/6.56	2.07/2.46/1.33
SL	Marker35344-Marker35422	3.42/6.86/6.82/8.05/8.05/8.83/4.82/4.43/7.43	6.84/11.15/9.46/10.91/14.89/13.41/6.18/8.31/13.51	0.46/0.6/0.66/0.76/0.75/0.7/0.53/0.48/0.58
	Marker69427-Marker69525	2.59/6/2.61	3.47/7.8/4.22	-0.36/-0.6/-0.32
	Marker81580-Marker81513	2.99/3.06/2.87/2.51	5.96/4.76/3.79/4.04	0.43/0.39/0.42/0.32
	Marker91133-Marker91933	4.62/3	5.9/5.63	-0.54/-0.39
SNS	Marker15740-Marker17413	16.86/4.13/6.11/5.4	16.18/7.47/9.85/8.21	0.82/0.35/0.4/0.25
	Marker23471-Marker23475	5.65/4.49	8.39/6.77	-0.5/-0.22
	Marker57882-Marker57915	2.51/4.94/5.3/5.63	2.34/10.46/9.69/9.68	-0.31/-0.41/-0.39/-0.27
	Marker103527-Marker103903	3.25/4.47	5.06/8.18	0.28/0.3

PVE mean of phenotypic variation explained, LOD logarithm of the odd, Add additive effect (Positive values indicate that the alleles from CM39 increases the trait scores, and negative values indicate that the allele from CM42 increases the trait scores), BLUP best linear unbiased prediction, Chr. chromosome, Env. environment

Marker35164 and Marker35422 (Table 2). Two QTL clusters were identified on chromosome 6A. One comprised two QTLs, *QTgw.cib-6A.1* and *QGl.cib-6A*, was located between Marker87546 and Marker87738 (Table 2). The other one contained five QTLs, *QTgw.cib-6A.2*, *QGw.cib-6A*, *QPh.cib-6A*, *QGns.cib-6A* and *QSl.cib-6A*, was located between Marker90210 and Marker91587 (Table 2).

Discussion

QTL analysis and comparison with previous studies

Wheat yield-related traits are significantly associated with yield and typically show higher heritability than the yield itself, and thus, mining the genes or QTLs related to yield-related traits will be help for elucidating the genetic

basis of wheat yield and facilitating the genetic improvement of varieties with high yield [5–7]. In the present study, a RIL population derived from two elite winter wheat varieties were used to dissect the genetic basis of variation for seven yield-related traits, including TGW, GNS, GW, GL, PH, SL and SNS. A total of 30 QTLs were identified in multiple environments, explaining 2.34–23.75% of the phenotypic variance (Table 2).

Fourteen QTLs were identified for grain size and weight, including two for TGW, six for GW and six for GL. Among them, *QTgw.cib-6A.1* and *QGl.cib-6A* were co-located on chromosome arm 6AS, which was near to *QTKw-6A.1* and *QTgw.cau-6A.4* [1, 43]. *QTgw.cib-6A.2* was located on chromosome arm 6AL and near to

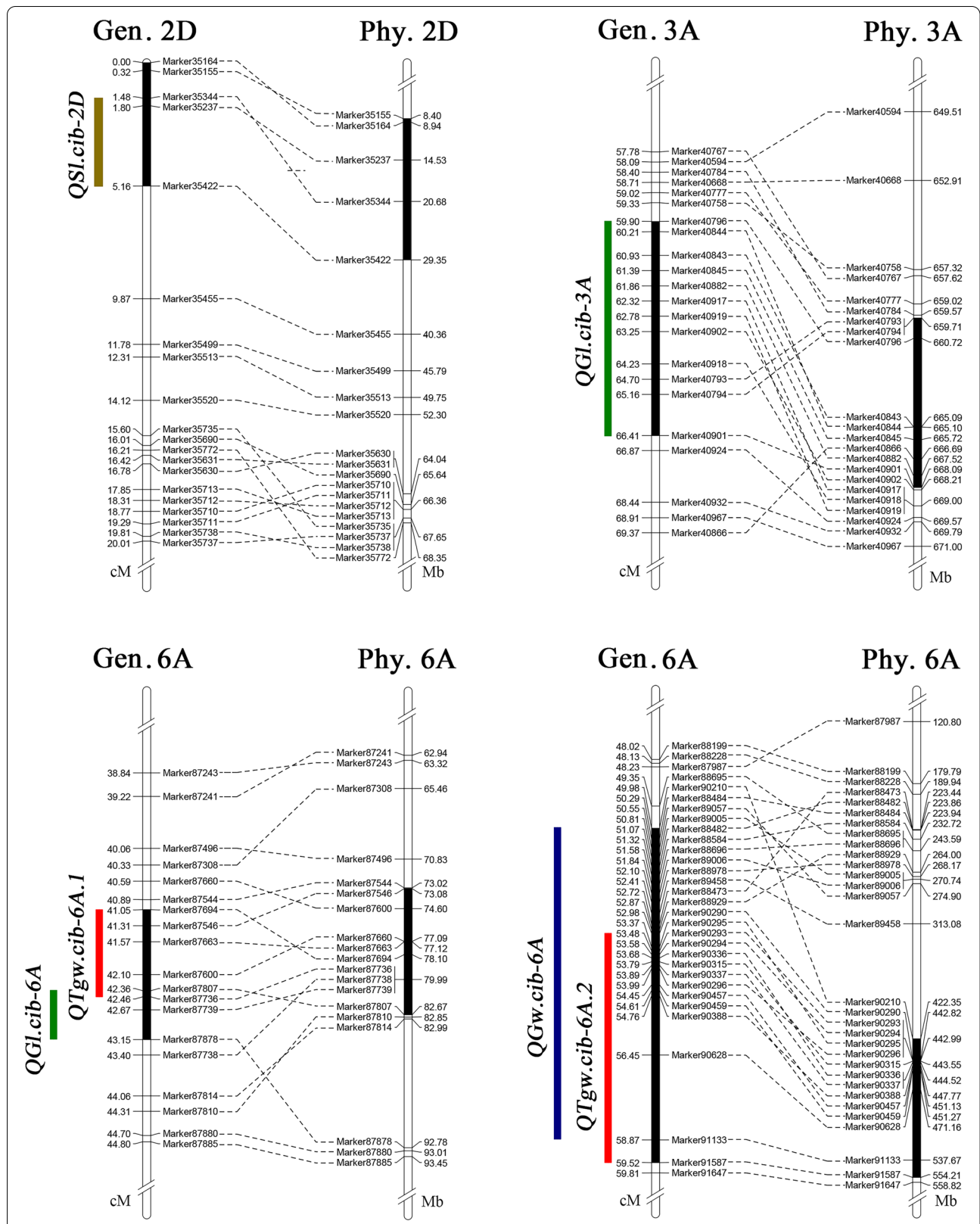
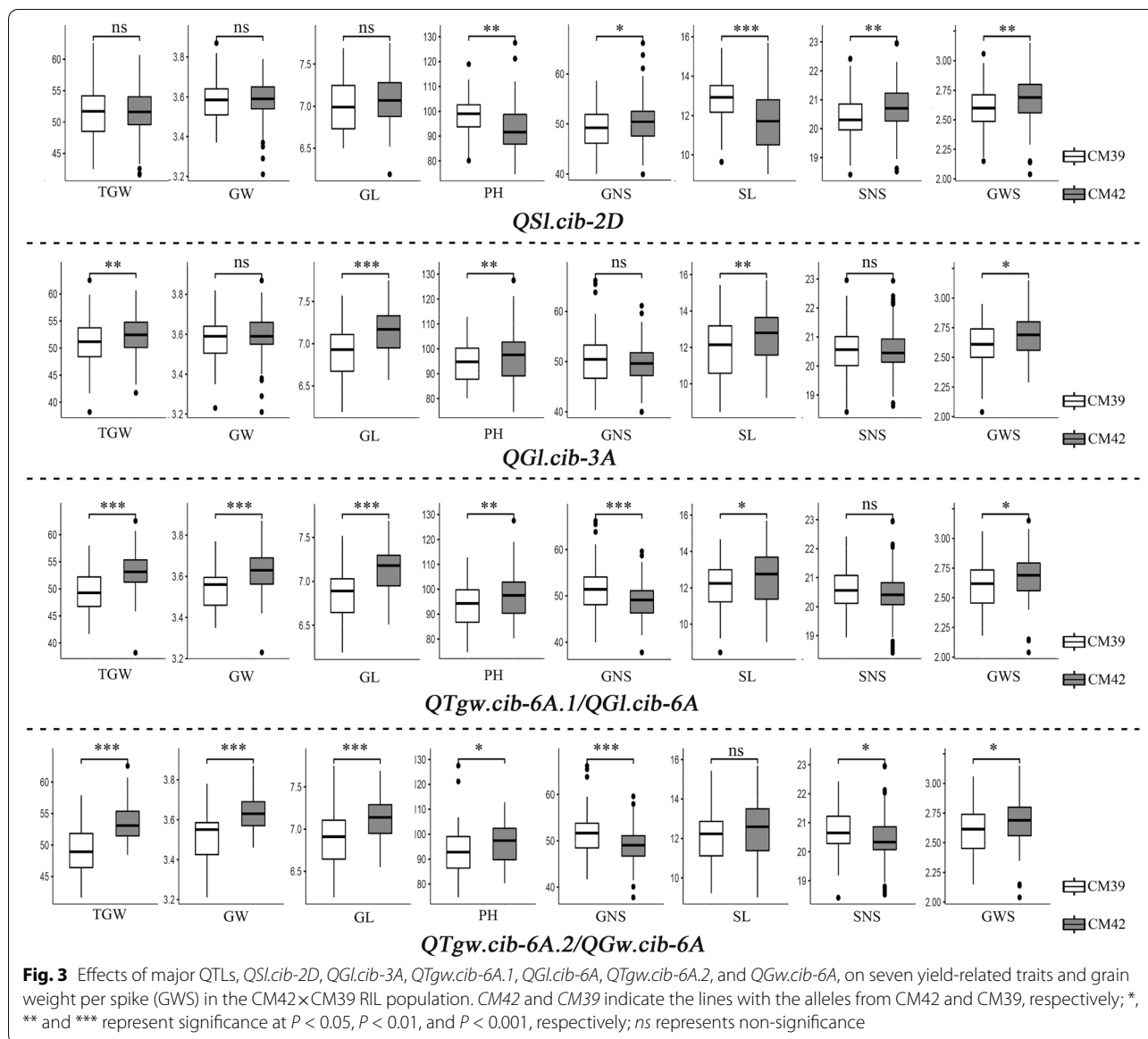


Fig. 2 The genetic and physical position of six major QTLs, *QSL.cib-2D*, *QGL.cib-3A*, *QTgw.cib-6A.1*, *QTgw.cib-6A.2*, *QGw.cib-6A*, and *QGL.cib-6A* detected in the CM42 x CM39 RIL population; *Chr.*, genetic position; *Phy.*, physical position



QTKW.caas-6AL and *QTKW-6A.1* [44, 45]. The QTL *QGw.cib-6A* for GW was located in a large interval on chromosome 6A. This interval was near to a known gene *TaGW2* controlling TGW and GW [46, 47]. *QGw.cib-2A* on chromosome 2A was overlapped with *QGwt.crc-2A* detected by McCartney et al [48]. *QGw.cib-2B.1* on chromosome 2B was overlapped with *qKW2B-1* detected by Xin et al [30]. *QGw.cib-7B* on chromosome 7B was located near to a QTL for TGW *QTgw.wa-7BL* [6]. Two QTLs for GL *QGl.cib-3A* and *QGl.cib-5A.1* on chromosomes 3A and 5A, respectively, were overlapped with two QTLs for GL detected by Mohler et al [49]. *QGl.cib-5A.2* was near to a QTL for TGW *QTKW.ndsu.5A.1* reported previously [47]. *QGl.cib-7D* was overlapped with *QGl*.

cau-7D detected by Yan et al [50]. For the rest three QTLs *QGw.cib-2B.2*, *QGw.cib-5A* and *QGl.cib-6D*, no stable QTL for grain size reported previously was overlapped with them, indicating they are likely novel QTL (Table 3).

PH and SL are important traits related to plant architecture and yield potential in wheat [12, 56]. In the present study, six and four QTLs for PH and SL were identified, respectively. Among them, *QPh.cib-2D* and *QSl.cib-2D* were co-located in the same interval on chromosome arm 2DS, which was overlapped with the dwarfing gene *Rht8* [31, 51]. *QPh.cib-4A* and *QPh.cib-5A* were located near to two loci for PH reported by Luján Basile et al [52]. *QPh.cib-6A* on chromosome 6A

Table 3 The physical interval of QTL detected in the present study and comparison with previously studies.

Trait	QTL	Chromosome	Physical position (Mb)	Nearby known locus	Reference
TGW	<i>QTgw.cib-6A.1</i>	6A	73.08-82.67	<i>QTKw-6A.1, QTgw.cau-6A.4</i>	[1, 43]
	<i>QTgw.cib-6A.2</i>	6A	442.82-554.21	<i>QTKW.caas-6AL, QTKW-6A.1</i>	[44, 45]
GW	<i>QGw.cib-2A</i>	2A	517.02-581.44	<i>QGwt.crc-2A</i>	[48]
	<i>QGw.cib-2B.1</i>	2B	150.75-151.74	<i>qKW2B-1</i>	[30]
	<i>QGw.cib-2B.2</i>	2B	734.72-734.72		
	<i>QGw.cib-5A</i>	5A	202.92-212.92		
	<i>QGw.cib-6A</i>	6A	422.35-537.67	<i>TaGW2</i>	[46, 47]
	<i>QGw.cib-7B</i>	7B	735.93-740.06	<i>QTgw.wa-7BL</i>	[6]
GL	<i>QGl.cib-3A</i>	3A	659.71-668.09	<i>IWA4298-IWB11347</i>	[49]
	<i>QGl.cib-5A.1</i>	5A	26.14-29.28	<i>IWA4871-IWB34408</i>	[49]
	<i>QGl.cib-5A.2</i>	5A	453.5-453.6	<i>QTKW.ndsu.5A.1</i>	[47]
	<i>QGl.cib-6A</i>	6A	79.99-82.67		
	<i>QGl.cib-6D</i>	6D	75.08-83.92		
	<i>QGl.cib-7D</i>	7D	66.19-107.61	<i>QGl.cau-7D</i>	[50]
PH	<i>QPh.cib-1A</i>	1A	345.37-443.28		
	<i>QPh.cib-2D</i>	2D	20.68-29.35	<i>Rht8, QPLH-2D</i>	[31, 51]
	<i>QPh.cib-4A</i>	4A	704.53-704.58	<i>Chr4A-B57-Hap6</i>	[52]
	<i>QPh.cib-5A</i>	5A	501.62-523.22	<i>Chr5A-B54-Hap3</i>	[52]
	<i>QPh.cib-5B</i>	5B	607.07-608.06		
	<i>QPh.cib-6A</i>	6A	447.77-451.27	<i>Rht18</i>	[53]
GNS	<i>QGns.cib-2D</i>	2D	8.4-29.35	<i>Rht8</i>	[31, 51]
	<i>QGns.cib-6A</i>	6A	471.16-554.21	<i>QTKW.caas-6AL, QTKW-6A.1</i>	[44, 45]
SL	<i>QSl.cib-2D</i>	2D	20.68-29.35	<i>Rht8, QPLH-2D</i>	[31, 51]
	<i>QSl.cib-5A</i>	5A	35.84-45.91	<i>QSL5A.3</i>	[54]
	<i>QSl.cib-5B</i>	5B	404.42-406.31		
	<i>QSl.cib-6A</i>	6A	537.67-584		
SNS	<i>Qsns.cib-1B</i>	1B	381.92-439.8	<i>QSn.sau-1BL</i>	[5]
	<i>Qsns.cib-1D</i>	1D	482.32-485.76		
	<i>Qsns.cib-4A</i>	4A	691.53-703.17		
	<i>Qsns.cib-7A</i>	7A	524.95-562.63	<i>QSn-7A.2</i>	[55]

was overlapped with the dwarfing gene *Rht18* [53]. *QSl.cib-5A* on chromosome 5A was located near to *QSL5A.3* detected by Liu et al [54]. For the rest four QTLs *QPh.cib-1A*, *QPh.cib-5B*, *QSl.cib-5B* and *QSl.cib-6A*, no stable QTL for PH and SL reported previously was overlapped with them, indicating they are likely novel (Table 3).

Two QTLs for GNS and four QTLs for SNS were identified in the present study. Of them, *QGns.cib-2D* were co-located with *QPh.cib-2D* and *QSl.cib-2D* on chromosome 2D and overlapped with the dwarfing gene *Rht8* [31, 51]. *QGns.cib-6A* was co-located with *QTgw.cib-6A.2* and near to two QTLs for TGW *QTKW.caas-6AL* and *QTKW-6A.1* [44, 45]. *Qsns.cib-1B* for SNS on chromosome 1B was overlapped with the *QSn.sau-1BL* reported recently [5]. *Qsns.cib-7A* for SNS on chromosome 7A was overlapped with *QSn-7A.2* detected by Cao et al [55]. For the rest two QTLs *Qsns.cib-1D* and *Qsns.cib-4A*, no

stable QTL for SNS reported previously was overlapped with them, indicating they are likely novel (Table 3).

QTL cluster on chromosomes 2D and 6A

Numerous co-located QTLs associated with multiple traits have been reported in the previous studies [2, 5, 24, 57, 58], which are beneficial to improve breeding efficiency for multiple elite traits, and thus is favorable for pyramiding breeding. In the present study, three QTLs *QSl.cib-2D*, *QPh.cib-2D* and *QGns.cib-2D* were co-located in the interval of 8.4-29.35 Mb on chromosome arm 2DS (Table 2). The allele of CM42 at the locus decreases SL and PH while increasing GNS. Additionally, the locus was overlapped with the dwarfing gene *Rht8*, which has been reported to associated with QTLs for PH, SL, SNS, GNS, spikelet compactness, TGW, and grain yield [12, 51, 59–61]. Interestingly, no QTL

for grain size and weight detected in the present study was overlapped with the locus, indicating it had no effect on grain size and weight. Given CM42 was bred by utilizing synthetic wheat germplasm [62], further studies, such as fine-mapping and map-based cloning are needed to future reveal the relationship between the locus and *Rht8*. However, the results in this study showed that the locus could be utilized in optimization PH with no penalty for grain size and weight in MAS.

Two QTL clusters were detected on chromosome 6A in the present study. One comprised two QTLs, *QTgw.cib-6A.1* and *QGl.cib-6A*, was located on chromosome arm 6AS (Table 2, Fig. 2). The other one comprised five QTLs, *QTgw.cib-6A.2*, *QGw.cib-6A*, *QGns.cib-6A*, *QPh.cib-6A*, and *QSl.cib-6A*, was located on chromosome arm 6AL (Table 2, Fig. 2). The QTL cluster on chromosome 6AL was overlapped with the haplotype block encompassing *TaGW2* and additional 2167 genes which was located between 187 Mb and 455 Mb on chromosome 6A and defined by Brinton et al [63]. Therefore, fine-mapping and map-based cloning is needed to dissect the relationships between *TaGW2* and the QTL cluster on chromosome 6AL in the future study. For the QTL cluster on chromosome 6AS, which was located between 73.08 Mb and 82.67 Mb and far apart the haplotype block of *TaGW2* [63], indicating that they are different loci for grain weight.

Additive effects of three major QTLs on TGW and GNS

Due to there is a trade-off between TGW and GNS, increasing one of them may not contribute to an increase in grain yield of wheat. We further analyzed the additive effects of three major QTLs, *QPh/Sl.cib-2D*, *QGl.cib-3A* and *QTgw.cib-6A.2*, on the TGW and GNS. As showed in the Table 4, lines possessing the allele from CM42 at the three loci had relatively higher TGW and GNS, which might partly explain the high yield of CM42. Additionally, lines possessing the alleles from CM42 at *QPh/*

Sl.cib-2D and *QTgw.cib-6A.2* and the allele from CM39 at *QGl.cib-3A* also had relatively higher TGW and GNS. However, for the other combination schemes, either the higher TGW but lower GNS, or higher GNS but lower TGW, or both lower TGW and GNS were harvested. Overall, the QTLs and KASP markers in this study will be useful for elucidating the genetic architecture of grain yield and developing new wheat varieties with high and stable yield in wheat.

aa, *bb* and *cc* represent the allele from CM39 at *QPh/Sl.cib-2D*, *QGl.cib-3A* and *QTgw.cib-6A.2*, respectively; *AA*, *BB* and *CC* represent the allele from CM42 at *QPh/Sl.cib-2D*, *QGl.cib-3A* and *QTgw.cib-6A.2*, respectively; *Lines* represent the number of different haplotypes; * and ** represent significance at $P < 0.05$ and $P < 0.01$, respectively; The superscript letter indicates significant difference among groups

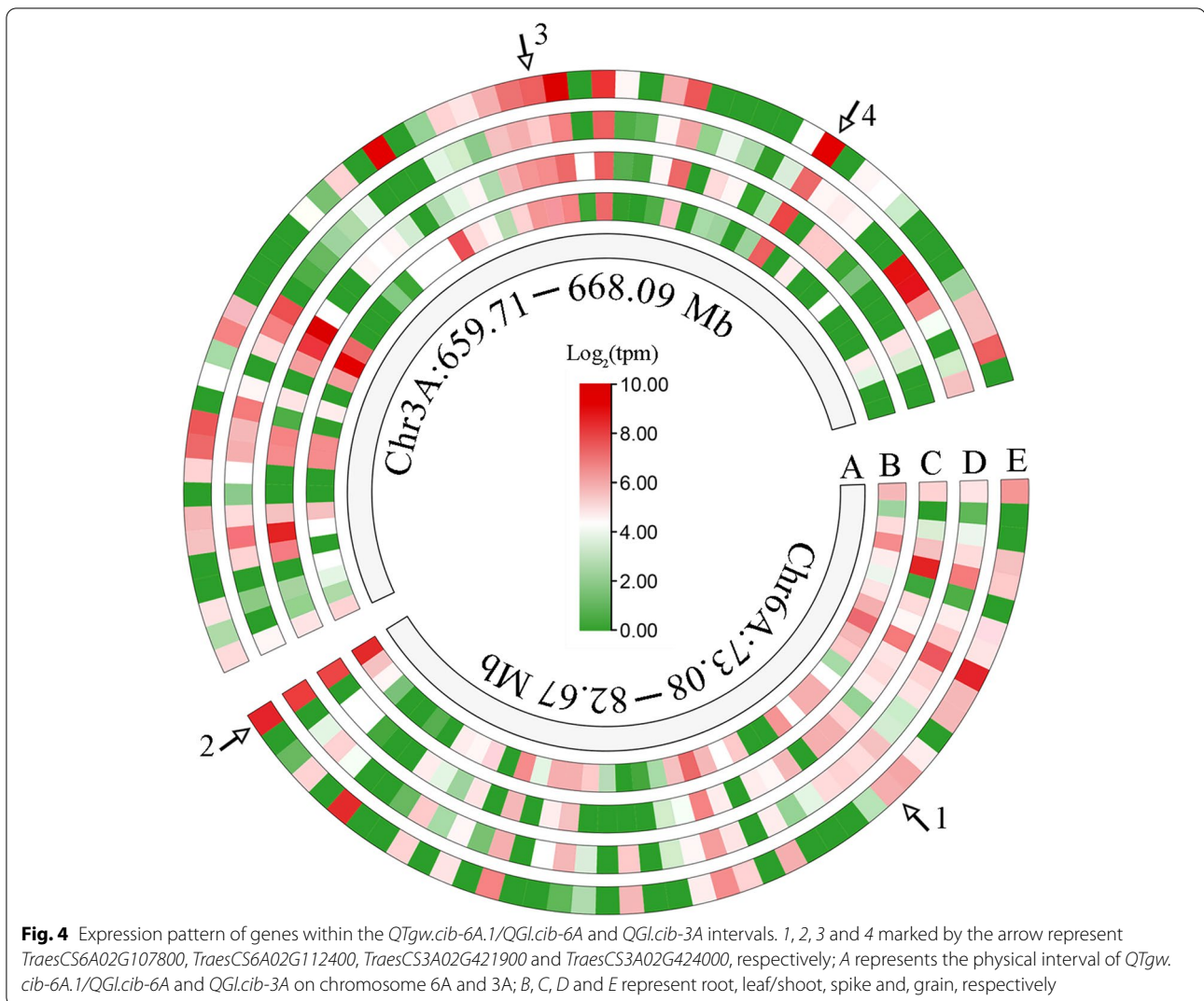
Potential candidate genes for *QTgw.cib-6A.1/QGl.cib-6A* and *QGl.cib-3A*

Among these major QTL, *QSl.cib-2D* is likely allele with *Rht8*. In the previous study, *TraesCS2D01G055700* was reported by Chai et al [64] as a possible candidate gene of *Rht8*. *QTgw.cib-6A.2/QGw.cib-6A* was needed additional populations to narrow their physical interval. Therefore, we mainly analyzed possible candidates for *QTgw.cib-6A.1/QGl.cib-6A* and *QGl.cib-3A* in the present study.

QTgw.cib-6A.1 and *QGl.cib-6A* were co-located between 73.08 and 82.67 Mb on Chinese Spring (CS) chromosome arm 6AS, and *QGl.cib-3A* was located between 659.71 and 668.09 Mb on CS chromosome arm 3AL (Table 3, Fig. 2). In the interval of *QTgw.cib-6A.1/QGl.cib-6A* and *QGl.cib-3A*, there were 81 and 85 predicted genes in the CS genome, respectively (Table S6, S7). Expression pattern analyses showed that 45 and 57 genes in the interval of *QTgw.cib-6A.1/QGl.cib-6A* and *Gl.cib-3A* expressed in various tissue, respectively (Fig. 4) [65, 66]. Among them, several were abundantly expressed in grain, indicating they are likely associated with grain growth and development (Fig. 4). For example, *TraesCS6A02G107800* is an ortholog of the rice *RGG2* and encodes a guanine nucleotide-binding protein subunit gamma 2 (Table S6). Miao et al previously reported that *RGG2* played a negative role in plant growth and yield production and that manipulation of *RGG2* can increase the plant biomass, grain weight, length and yield in rice [67]. *TraesCS6A02G112400* and *TraesCS3A02G424000* encode polyubiquitin and small ubiquitin-related modifier, respectively (Table S6, S7). *TraesCS3A02G421900* encodes a 26S proteasome regulatory subunit (Table S7), which participates in the ubiquitin/26S proteasome pathway and mediate the degradation of the complex of ubiquitin receptor and poly-ubiquitinated protein [68, 69].

Table 4 Analyses of additive effects on TGW and GNS of three major QTLs *QPh/Sl.cib-2D*, *QGl.cib-3A* and *QTgw.cib-6A.2*

QTL	Lines	TGW(g) **	GNS *
aabbcc	20	46.97±2.85 ^a	52.25±5.25 ^{cd}
AABBcc	14	47.63±3.29 ^a	49.78±5.12 ^{abc}
AAbbcc	7	49.75±3.76 ^{ab}	55.2±5.51 ^d
aaBBcc	16	51.53±2.42 ^{bc}	50.58±3.48 ^{bc}
aabbCC	20	53.13±3.49 ^{cd}	47.74±4.1 ^a
AAbbCC	18	53.17±2.17 ^{cd}	50.58±4 ^{bc}
aaBBCC	21	54.25±2.94 ^d	48.84±3.47 ^{ab}
AABBCC	31	53.32±2.88 ^d	50.07±2.86 ^{bc}



Previous studies revealed that the ubiquitin pathway play an important role in regulation grain size and weight in rice [70, 71]. These results indicated that the four genes may be closely related to grain size and weight in wheat and useful for fine mapping and cloning of *QTgw.cib-6A.1/QGL.cib-6A* and *QGL.cib-3A* in our following work.

Conclusion

In this study, a total of 30 QTLs for TGW, GNS, GW, GL, PH, SL, and SNS were identified, explaining 2.34–23.75% of the phenotypic variance. Among them, six major QTLs *QTgw.cib-6A.1*, *QTgw.cib-6A.2*, *QGw.cib-6A*, *QGL.cib-3A*, *QGL.cib-6A*, and *QSl.cib-2D* were detected. Three KASP markers linked with five of these major QTLs were developed. These QTLs and KASP markers will be useful for elucidating the genetic architecture of grain yield

and developing new wheat varieties with high and stable yield in wheat. Additionally, candidate genes of *QTgw.cib-6A.1/QGL.cib-6A* and *QGL.cib-3A* were preliminary analyzed.

Methods

Plant materials and field trials

A RIL population (F_{10}) comprising 193 lines derived from a cross CM42 and CM39 were used for QTL detection in the present study. CM42 is the first wheat elite variety in the world bred by using synthetic hexaploid wheat (*Triticum turgidum* × *Aegilops tauschii*) germplasm, and showed high yield potential in Sichuan and the Yangzi River region [62], while CM39 is an elite winter wheat variety with different genetic background to that of CM42. During four growing seasons of wheat

from 2015–2016 to 2018–2019, the RIL population along with their parents were evaluated at two experimental sites in Sichuan province of China, including Shuangliu (SHL, 103° 52'E, 30°34'N) and Shifang (SHE, 104°11'E, 31°6'N). Randomized block design was adopted for all of the trials. Each line was planted in a one-row plot with 50 seeds per row, a row length of 2.0 m, and a row spacing of 0.3 m. Five replicates were performed under each environment. Nitrogen and superphosphate fertilizers were applied at a rate of 80 and 100 kg/ha, respectively, at sowing. Crop management and disease control were performed according to local cultivation practices.

Phenotyping and statistical analysis

At maturity, ten representative plants from middle row of each line were randomly selected to investigate agronomic traits including TGW, GL, GW, GNS, PH, SL, SNS and GWS. SL was measured as the length from the base of the rachis to the tip of the terminal spikelet, excluding the awns. SNS was determined by counting the number of spikelets in main spikes; PH was measured from the soil surface to the tip of the spike, excluding the awns. Subsequently, the main spike of all selected plants were harvested and manually threshed for evaluating GNS, TGW, GW, GL and GWS using SC-G software (Wseen Co., Ltd, Hangzhou, China). PH and SL were evaluated in eight environments, and the rest traits were evaluated in six environments.

Basic phenotypic statistical analyses, frequency distribution, correlation analyses and student's t tests were performed with SPSS version 20.0 (Chicago, IL, USA). The phenotype distribution graph was drawn using the plugin "CorrPlot" in TBtools [72]. The relationships among measured traits were visualized using the R package "qgraph". The BLUP data across evaluated environments was calculated using the "lmer" function implemented in R package "lme4". ANOVA was performed over all trials which indicated statistically significant main effects for genotypes (G), environments (E), G × E interactions for all measured traits using the SAS software (SAS Institute Inc., North Carolina, USA). The broad sense heritability (H^2) was estimated based on the following equation: $H^2 = \sigma_g^2 / (\sigma_g^2 + \sigma_{ge}^2/n + \sigma_e^2/nr)$, where σ_g^2 is the variance of genotypes, σ_{ge}^2 is the variance of genotype by environmental effect, σ_e^2 is the residual variance, n is the number of environments and r is the number of replicates [73].

Linkage map construction and QTL detection

A whole-genome genetic map constructed previously was adopted for QTL mapping [42]. The genetic map was constructed using the CM42×CM39 RIL

population with SLAF markers. A total of 4996 Bin SLAFs were distributed in 21 linkage groups and covered a total genetic distance of 2,859.94 cM with an average interval of 0.57 cM between adjacent Bin marker (Table S1, S2) [42].

QTL analysis was conducted using the inclusive composite interval mapping (ICIM) function of IciMapping 4.1 (<https://www.isbreeding.net>) with the minimal LOD score was set at 2.5. The missing phenotype was deleted in QTL analysis. QTL was named according to the provision of Genetic Nomenclature (<http://wheat.pw.usda.gov/ggpages/wgc/98/Intro.htm>), where 'CIB' represents Chengdu Institute of Biology. QTLs consistently identified in at least three environments and in combined analysis with $\geq 10\%$ of phenotypic variation explained were considered as major QTLs.

Development of Kompetitive Allele-Specific PCR Markers

On the basis of the preliminary QTL mapping results, the flanking markers of major QTL were blasted against the CS reference genome sequence (RefSeq v1.0; <https://wheat-urgi.versailles.inra.fr/>) to gain their physical positions [74]. The SNPs within the physical interval of major QTLs were used for developing KASP markers tight linked with them. The KASP marker primers were designed using the PrimerServer tool in Triticeae Multi-omics Center (<http://202.194.139.32/>) [75]. Standard FAM and HEX adapters were added to the allele-specific forward primers at the 5' ends. The KASP assays were run in a Bio-Rad CFX96 real-time PCR system in 10 μ L reaction volumes with the following PCR cycling parameters: hot start enzyme activation at 94 °C for 15 min; a touchdown of 10 cycles (94 °C for 20 s, and touchdown starting at 61 °C and decreasing by 0.6 °C per 1-min cycle); then 26 cycles of regular PCR (94 °C for 20 s, 55 °C for 60 s, and rest at 37 °C for 1 min). If the clustering was not significant, further cycling was performed at 94 °C for 20 s and 55 °C for 60 s (3–10 cycles per step)

Prediction of candidate gene

Genes between the physical intervals of major QTLs were extracted from IWGSC RefSeq v1.1 annotation for CS [74]. The annotations and functions of a given gene were analyzed using UniProt (<https://www.uniprot.org/>). The expression pattern analysis was performed by using Wheat Expression Browser (<http://www.wheat-expression.com/>), and the circle graph of expression values was drawn using TBtools [72]. The orthologous gene analysis between wheat and rice was conducted using the Triticeae-Gene Tribe (<http://wheat.cau.edu.cn/TGT/>) [76].

Abbreviations

CM42: Chuanmai42; CM39: Chuanmai39; SHF: Shifang; SHL: Shuangliu; TGW : Thousand grain weight; GNS: Grain number per spike; GW: Grain width; GL: Grain length; PH: Plant height; SL: Spike length; SNS: Spikelet number per spike; QTL: Quantitative trait loci; SLAF: Specific-locus amplified fragment; MAS: Marker-assisted selection; KASP: Kompetitive Allele Specific PCR; BLUP: Best linear unbiased prediction; CS: Chinese Spring.

Supplementary Information

The online version contains supplementary material available at <https://doi.org/10.1186/s12863-022-01050-0>.

Additional file 1.

Additional file 2.

Acknowledgement

Not applicable.

Authors' contributions

TL undertook the field trials and subsequent analysis of all available data including the phenotyping and population genotyping, and drafted this manuscript. QL and ZP undertook the genetic map constructed. JW, ZY, YT, YS, JZ, XQ and XP participated in phenotyping. ZL, WY and JL developed and provided us the CC population. MY, JL, YW and HZ discussed results. HL and GD designed the experiments, guided the entire study, participated in data analysis, discussed results and revised the manuscript. The authors read and approved the final manuscript.

Funding

This work is supported by National Key R&D Program of China (2016YFD0100102), Strategic Priority Research Program of the Chinese Academy of Sciences (Grant No. XDA08020205), Science and Technology Support Project of Sichuan Province, China (2016NZ0103), Key Project of Crop Breeding of Sichuan Province (2016NYZ0030), and Science and technology projects of Sichuan Province (2020YFSY0049).

Availability of data and materials

All data used in this study was present in the manuscript and supporting materials.

Declarations

Ethical approval and consent to participate

Not applicable.

Consent for publication

Not applicable.

Competing interests

All authors declare that they have no conflict of interest.

Author details

¹Chengdu Institute of Biology, Chinese Academy of Sciences, Chengdu 610041, China. ²Triticeae Research Institute, Sichuan Agricultural University, Chengdu 611130, China. ³State Key Laboratory of Crop Gene Exploration and Utilization in Southwest China, Chengdu 611130, China. ⁴Crop Research Institute, Sichuan Academy of Agricultural Sciences, Chengdu 610066, Sichuan, China.

Received: 5 August 2021 Accepted: 6 April 2022

Published online: 13 May 2022

References

- Guan P, Lu L, Jia L, Kabir MR, Zhang J, Lan T, et al. Global QTL Analysis Identifies Genomic Regions on Chromosomes 4A and 4B Harboring Stable Loci for Yield-Related Traits Across Different Environments in Wheat (*Triticum aestivum* L.). *Front Plant Sci.* 2018;9:1–14.
- Isham K, Wang R, Zhao W, Wheeler J, Klassen N, Akhunov E, et al. QTL mapping for grain yield and three yield components in a population derived from two high-yielding spring wheat cultivars. *Theor Appl Genet.* 2021;134:2079–95.
- Li T, Deng G, Tang Y, Su Y, Wang J, Cheng J. Identification and Validation of a Novel Locus Controlling Spikelet Number in Bread Wheat (*Triticum aestivum* L.). *Front Plant Sci.* 2021;12:1–14.
- Cui F, Ding A, Li J, Zhao C, Wang L, Wang X, et al. QTL detection of seven spike-related traits and their genetic correlations in wheat using two related RIL populations. *Euphytica.* 2012;186:177–92.
- Ren T, Fan T, Chen S, Li C, Chen Y, Ou X, et al. Utilization of a Wheat55K SNP array-derived high-density genetic map for high-resolution mapping of quantitative trait loci for important kernel-related traits in common wheat. *Theor Appl Genet.* 2021;134:807–21.
- Wang J, Liu W, Wang H, Li L, Wu J, Yang X, et al. QTL mapping of yield-related traits in the wheat germplasm 3228. *Euphytica.* 2011;177:277–92.
- Chu CG, Xu SS, Friesen TL, Faris JD. Whole genome mapping in a wheat doubled haploid population using SSRs and TRAPs and the identification of QTL for agronomic traits. *Mol Breed.* 2008;22:251–66.
- Ellis MH, Spielmeier W, Gale KR, Rebetzke GJ, Richards RA. "Perfect" markers for the Rht-B1b and Rht-D1b dwarfing genes in wheat. *Theor Appl Genet.* 2002;105:1038–42.
- Lv C, Song Y, Gao L, Yao Q, Zhou R, Xu R, et al. Integration of QTL detection and marker assisted selection for improving resistance to Fusarium head blight and important agronomic traits in wheat. *Crop J.* 2014;2:70–8.
- Du Y, Chen L, Wang Y, Yang Z, Saeed I, Daoura BG, et al. The combination of dwarfing genes Rht4 and Rht8 reduced plant height, improved yield traits of rainfed bread wheat (*Triticum aestivum* L.). *F Crop Res.* 2018;215:149–55.
- Fan X, Cui F, Ji J, Zhang W, Zhao X, Liu JJ, et al. Dissection of pleiotropic QTL regions controlling wheat spike characteristics under different nitrogen treatments using traditional and conditional QTL mapping. *Front Plant Sci.* 2019;10:1–13.
- Zhai H, Feng Z, Li J, Liu X, Xiao S, Ni Z, et al. QTL analysis of spike morphological traits and plant height in winter wheat (*Triticum aestivum* L.) using a high-density SNP and SSR-based linkage map. *Front Plant Sci.* 2016;7:1–13.
- Cheng X, Xin M, Xu R, Chen Z, Cai W, Chai L, et al. A single amino acid substitution in STKc_GSK3 kinase conferring semispherical grains and its implications for the origin of triticum sphaerococcum. *Plant Cell.* 2020;32:923–34.
- Chen Y, Yan Y, Wu TT, Zhang GL, Yin H, Chen W, et al. Cloning of wheat keto-acyl thiolase 2B reveals a role of jasmonic acid in grain weight determination. *Nat Commun.* 2020;11:6266.
- Dobrovolskaya O, Pont C, Sibout R, Martinek P, Badaeva E, Murat F, et al. Frizzy panicle drives supernumerary spikelets in bread wheat. *Plant Physiol.* 2015;167:189–99.
- Voss-Fels KP, Keeble-Gagnère G, Hickey LT, Tibbits J, Nagorny S, Hayden MJ, et al. High-resolution mapping of rachis nodes per rachis, a critical determinant of grain yield components in wheat. *Theor Appl Genet.* 2019;132:2707–19.
- Yang Z, Bai Z, Li X, Wang P, Wu Q, Yang L, et al. SNP identification and allelic-specific PCR markers development for TaGW2, a gene linked to wheat kernel weight. *Theor Appl Genet.* 2012;125:1057–68.
- Zhang L, Zhao YL, Gao LF, Zhao GY, Zhou RH, Zhang BS, et al. TaCKX6-D1, the ortholog of rice OsCKX2, is associated with grain weight in hexaploid wheat. *New Phytol.* 2012;195:574–84.
- Hanif M, Gao F, Liu J, Wen W, Zhang Y, Rasheed A, et al. TaTGW6-A1, an ortholog of rice TGW6, is associated with grain weight and yield in bread wheat. *Mol Breed.* 2016;36:1–8.
- Dong L, Wang F, Liu T, Dong Z, Li A, Jing R, et al. Natural variation of TaGASR7-A1 affects grain length in common wheat under multiple cultivation conditions. *Mol Breed.* 2014;34:937–47.
- Yang J, Zhou Y, Wu Q, Chen Y, Zhang P, Zhang Y, et al. Molecular characterization of a novel TaGL3-5A allele and its association with grain length in wheat (*Triticum aestivum* L.). *Theor Appl Genet.* 2019;132:1799–814.
- Zhang Y, Liu J, Xia X, He Z. TaGS-D1, an ortholog of rice OsGS3, is associated with grain weight and grain length in common wheat. *Mol Breed.* 2014;34:1097–107.

23. Wang W, Pan Q, Tian B, He F, Chen Y, Bai G, et al. Gene editing of the wheat homologs of TONNEAU1-recruiting motif encoding gene affects grain shape and weight in wheat. *Plant J.* 2019;100:251–64.
24. Cao S, Xu D, Hanif M, Xia X, He Z. Genetic architecture underpinning yield component traits in wheat. *Theor Appl Genet.* 2020;133:1811–23.
25. Okamoto Y, Nguyen AT, Yoshioka M, Iehisa JCM, Takumi S. Identification of quantitative trait loci controlling grain size and shape in the D genome of synthetic hexaploid wheat lines. *Breed Sci.* 2013;63:423–9.
26. Marza F, Bai GH, Carver BF, Zhou WC. Quantitative trait loci for yield and related traits in the wheat population Ning7840 x Clark. *Theor Appl Genet.* 2006;112:688–98.
27. Liu T, Wu L, Gan X, Chen W, Liu B, Fedak G, et al. Mapping quantitative trait loci for 1000-grain weight in a double haploid population of common wheat. *Int J Mol Sci.* 2020;21:3960.
28. Li X, Xia X, Xiao Y, He Z, Wang D, Trethowan R, et al. QTL mapping for plant height and yield components in common wheat under water-limited and full irrigation environments. *Crop Pasture Sci.* 2015;66:660–70.
29. Su Q, Zhang X, Zhang W, Zhang N, Song L, Liu L, et al. QTL Detection for Kernel Size and Weight in Bread Wheat (*Triticum aestivum* L.) Using a High-Density SNP and SSR-Based Linkage Map. *Front. Plant Sci.* 2018;9:1–13.
30. Xin F, Zhu T, Wei S, Han Y, Zhao Y, Zhang D, et al. QTL Mapping of Kernel Traits and Validation of a Major QTL for Kernel Length-Width Ratio Using SNP and Bulk Segregant Analysis in Wheat. *Sci Rep.* 2020;10:1–12.
31. Mohan A, Grant NP, Schillinger WF, Gill KS. Characterizing reduced height wheat mutants for traits affecting abiotic stress and photosynthesis during seedling growth. *Physiol Plant.* 2021;172:233–46.
32. Mo Y, Vanzetti LS, Hale I, Spagnolo EJ, Guidobaldi F, Al-Oboudi J, et al. Identification and characterization of Rht25, a locus on chromosome arm 6AS affecting wheat plant height, heading time, and spike development. *Theor Appl Genet.* 2018;131:2021–35.
33. Guan P, Shen X, Mu Q, Wang Y, Wang X, Chen Y, et al. Dissection and validation of a QTL cluster linked to Rht-B1 locus controlling grain weight in common wheat (*Triticum aestivum* L.) using near-isogenic lines. *Theor Appl Genet.* 2020;133:2639–53.
34. Duan X, Yu H, Ma W, Sun J, Zhao Y, Yang R, et al. A major and stable QTL controlling wheat thousand grain weight: identification, characterization, and CAPS marker development. *Mol Breed.* 2020;40:68.
35. Chen W, Sun D, Li R, Wang S, Shi Y, Zhang W, et al. Mining the stable quantitative trait loci for agronomic traits in wheat (*Triticum aestivum* L.) based on an introgression line population. *BMC Plant Biol.* 2020;20:1–9.
36. Maccaferri M, Ricci A, Salvi S, Milner SG, Noli E, Martelli PL, et al. A high-density, SNP-based consensus map of tetraploid wheat as a bridge to integrate durum and bread wheat genomics and breeding. *Plant Biotechnol J.* 2015;13:648–63.
37. Li T, Deng G, Su Y, Yang Z, Tang Y, Wang J, et al. Identification and validation of two major QTLs for spike compactness and length in bread wheat (*Triticum aestivum* L.) showing pleiotropic effects on yield-related traits. *Theor Appl Genet.* 2021;134:3625–41.
38. Li T, Deng G, Su Y, Yang Z, Tang Y, Wang J, et al. Genetic dissection of quantitative trait loci for grain size and weight by high-resolution genetic mapping in bread wheat (*Triticum aestivum* L.). *Theor Appl Genet.* 2022;135:257–71.
39. Wang F, Zhang J, Chen Y, Zhang C, Gong J, Song Z, et al. Identification of candidate genes for key fibre-related QTLs and derivation of favourable alleles in *Gossypium hirsutum* recombinant inbred lines with *G. barbadense* introgressions. 2020:707–20.
40. Ma J, Pei W, Ma Q, Geng Y, Liu G, Liu J, et al. QTL analysis and candidate gene identification for plant height in cotton based on an interspecific backcross inbred line population of *Gossypium hirsutum* x *Gossypium barbadense*. *Theor Appl Genet.* 2019;132:2663–76.
41. Han J, Han D, Guo Y, Yan H, Wei Z, Tian Y, et al. QTL mapping pod dehiscence resistance in soybean (*Glycine max* L. Merr.) using specific-locus amplified fragment sequencing. *Theor Appl Genet.* 2019;132:2253–72.
42. Li Q, Pan Z, Gao Y, Li T, Liang J, Zhang Z, et al. Quantitative Trait Locus (QTLs) Mapping for Quality Traits of Wheat Based on High Density Genetic Map Combined With Bulk Segregant Analysis RNA-seq (BSR-Seq) Indicates That the Basic 7S Globulin Gene Is Related to Falling Number. *Front Plant Sci.* 2020;11:1–21.
43. Cui F, Zhao C, Ding A, Li J, Wang L, Li X, et al. Construction of an integrative linkage map and QTL mapping of grain yield-related traits using three related wheat RIL populations. *Theor Appl Genet.* 2014;127:659–75.
44. Li F, Wen W, He Z, Liu J, Jin H, Cao S, et al. Genome-wide linkage mapping of yield-related traits in three Chinese bread wheat populations using high-density SNP markers. *Theor Appl Genet.* 2018;131:1903–24.
45. Lee HS, Jung JU, Kang CS, Heo HY, Park CS. Mapping of QTL for yield and its related traits in a doubled haploid population of Korean wheat. *Plant Biotechnol Rep.* 2014;8:443–54.
46. Maphosa L, Langridge P, Taylor H, Parent B, Emebiri LC, Kuchel H, et al. Genetic control of grain yield and grain physical characteristics in a bread wheat population grown under a range of environmental conditions. *Theor Appl Genet.* 2014;127:1607–24.
47. Kumar A, Mantovani EE, Seetan R, Soltani A, Echeverry-Solarte M, Jain S, et al. Dissection of Genetic Factors underlying Wheat Kernel Shape and Size in an Elite x Nonadapted Cross using a High Density SNP Linkage Map. *Plant Genome.* 2016;9.
48. McCartney CA, Somers DJ, Humphreys DG, Lukow O, Ames N, Noll J, et al. Mapping quantitative trait loci controlling agronomic traits in the spring wheat cross RL4452 x "AC Domain". *Genome.* 2005;48:870–83.
49. Mohler V, Albrecht T, Castell A, Diethelm M, Schweizer G, Hartl L. Considering causal genes in the genetic dissection of kernel traits in common wheat. *J Appl Genet.* 2016;57:467–76.
50. Daba SD, Tyagi P, Brown-Guedira G, Mohammadi M. Genome-wide association study in historical and contemporary U.S. winter wheats identifies height-reducing loci. *Crop J.* 2020;8:243–51.
51. Luján Basile SM, Ramírez IA, Crescente JM, Conde MB, Demichelis M, Abbate P, et al. Haplotype block analysis of an Argentinean hexaploid wheat collection and GWAS for yield components and adaptation. *BMC Plant Biol.* 2019;19:1–16.
52. Ford BA, Foo E, Sharwood R, Karafiatova M, Vrána J, MacMillan C, et al. Rht18 Semidwarfism in Wheat Is Due to Increased GA 2-oxidaseA9 Expression and Reduced GA Content. *Plant Physiol.* 2018;177:168–80.
53. Liu K, Sun X, Ning T, Duan X, Wang Q, Liu T, et al. Genetic dissection of wheat panicle traits using linkage analysis and a genome-wide association study. *Theor Appl Genet.* 2018;131:1073–90.
54. Cao P, Liang X, Zhao H, Feng B, Xu E, Wang L, et al. Identification of the quantitative trait loci controlling spike-related traits in hexaploid wheat (*Triticum aestivum* L.). *Planta.* 2019;250:1967–81.
55. Tian X, Wen W, Xie L, Fu L, Xu D, Fu C, et al. Molecular mapping of reduced plant height gene Rht24 in bread wheat. *Front Plant Sci.* 2017;8:1–9.
56. Ma J, Tu Y, Zhu J, Luo W, Liu H, Li C, et al. Flag leaf size and posture of bread wheat: genetic dissection, QTL validation and their relationships with yield-related traits. *Theor Appl Genet.* 2020;133:297–315.
57. Gao F, Wen W, Liu J, Rasheed A, Yin G, Xia X, et al. Genome-Wide Linkage Mapping of QTL for Yield Components, Plant Height and Yield-Related Physiological Traits in the Chinese Wheat Cross Zhou 8425B/Chinese Spring. *Front Plant Sci.* 2015;6:1099.
58. Zhang K, Wang J, Qin H, Wei Z, Hang L, Zhang P, et al. Assessment of the individual and combined effects of Rht8 and Ppd-D1a on plant height, time to heading and yield traits in common wheat. *Crop J.* 2019;7:845–56.
59. Rebetzke GJ, Ellis MH, Bonnett DG, Mickelson B, Condon AG, Richards RA. Height reduction and agronomic performance for selected gibberellin-responsive dwarfing genes in bread wheat (*Triticum aestivum* L.). *F Crop Res.* 2012;126:87–96.
60. Wang Y, Du Y, Yang Z, Chen L, Condon AG, Hu YG. Comparing the effects of GA-responsive dwarfing genes Rht13 and Rht8 on plant height and some agronomic traits in common wheat. *F Crop Res.* 2015;179:35–43.
61. Yang W, Liu D, Li J, Zhang L, Wei H, Hu X, et al. Synthetic hexaploid wheat and its utilization for wheat genetic improvement in China. *J Genet Genomics.* 2009;36:539–46.
62. Brinton J, Ramirez-Gonzalez RH, Simmonds J, Wingen L, Orford S, Griffiths S, et al. A haplotype-led approach to increase the precision of wheat breeding. *Commun Biol.* 2020;3:1–11.
63. Chai L, Chen Z, Bian R, Zhai H, Cheng X, Peng H, et al. Correction to: Dissection of two quantitative trait loci with pleiotropic effects on plant height and spike length linked in coupling phase on the short arm of chromosome 2D of common wheat (*Triticum aestivum* L.). *Theor Appl Genet.* 2019;132:3225.

65. Borrill P, Ramirez-Gonzalez R, Uauy C. expVIP: A customizable RNA-seq data analysis and visualization platform. *Plant Physiol.* 2016;170:2172–86.
66. Ramírez-González RH, Borrill P, Lang D, Harrington SA, Brinton J, Venturini L, et al. The transcriptional landscape of polyploid wheat. *Science.* 2018;361:eaar6089.
67. Miao J, Yang Z, Zhang D, Wang Y, Xu M, Zhou L, et al. Mutation of RGG2, which encodes a type B heterotrimeric G protein γ subunit, increases grain size and yield production in rice. *Plant Biotechnol J.* 2019;17:650–64.
68. Li N, Li Y. Ubiquitin-mediated control of seed size in plants. *Front Plant Sci.* 2014;5:1–6.
69. Smalle J, Kurepa J, Yang P, Emborg TJ, Babychuk E, Kushnir S, et al. The pleiotropic role of the 26S proteasome subunit RPN10 in Arabidopsis growth and development supports a substrate-specific function in abscisic acid signaling. *Plant Cell.* 2003;15:965–80.
70. Li N, Xu R, Li Y. Molecular Networks of Seed Size Control in Plants. *Annu Rev Plant Biol.* 2019;70:435–63.
71. Li Q, Li L, Yang X, Warburton ML, Bai G, Dai J, et al. Relationship, evolutionary fate and function of two maize co-orthologs of rice GW2 associated with kernel size and weight. *BMC Plant Biol.* 2010;10:1–15.
72. Chen C, Chen H, Zhang Y, Thomas HR, Frank MH, He Y, et al. TBtools: An Integrative Toolkit Developed for Interactive Analyses of Big Biological Data. *Mol Plant.* 2020;13:1194–202.
73. Smith SE, Kuehl RO, Ray IM, Hui R, Soleri D. Evaluation of simple methods for estimating broad-sense heritability in stands of randomly planted genotypes. *Crop Sci.* 1998;38:1125–9.
74. Appels R, Eversole K, Feuillet C, Keller B, Rogers J, Stein N, et al. Shifting the limits in wheat research and breeding using a fully annotated reference genome. *Science.* 2018;361:eaar7191.
75. Ma S, Wang M, Wu J, Guo W, Chen Y, Li G, et al. WheatOmics: A platform combining multiple omics data to accelerate functional genomics studies in wheat. *Mol Plant.* 2021;14:1965–8.
76. Chen Y, Song W, Xie X, Wang Z, Guan P, Peng H, et al. A Collinearity-Incorporating Homology Inference Strategy for Connecting Emerging Assemblies in the Triticeae Tribe as a Pilot Practice in the Plant Pangenomic Era. *Mol Plant.* 2020;13:1694–708.

Publisher's Note

Springer Nature remains neutral with regard to jurisdictional claims in published maps and institutional affiliations.

Ready to submit your research? Choose BMC and benefit from:

- fast, convenient online submission
- thorough peer review by experienced researchers in your field
- rapid publication on acceptance
- support for research data, including large and complex data types
- gold Open Access which fosters wider collaboration and increased citations
- maximum visibility for your research: over 100M website views per year

At BMC, research is always in progress.

Learn more biomedcentral.com/submissions

